A High Resolution Diagnostic Wind Model. Application to Downscaling Mesoscale Model Results for Wind Forecasting

SIANI
INSTITUTO UNIVERSITARIO
INGENIERIA COMPUTACIONAL

University Institute for Intelligent Systems and Numerical Applications in Engineering

6th European Conference on Computational Mechanics (Solids, Structures and Coupled Problems)
7th European Conference on Computational Fluid Dynamics
ECCM-ECFD 2017 – June, 2018, Glasgow

G. Montero, R. Montenegro, J.M. Escobar, E. Rodríguez, A. Oliver, A. Suárez

http://www.siani.es/

UNIVERSIDAD DE LAS PALMAS
DE GRAN CANARIA

Wind Field Modeling

Overview

Wind3D Code (freely-available)

http://www.dca.iusiani.ulpgc.es/Wind3D/

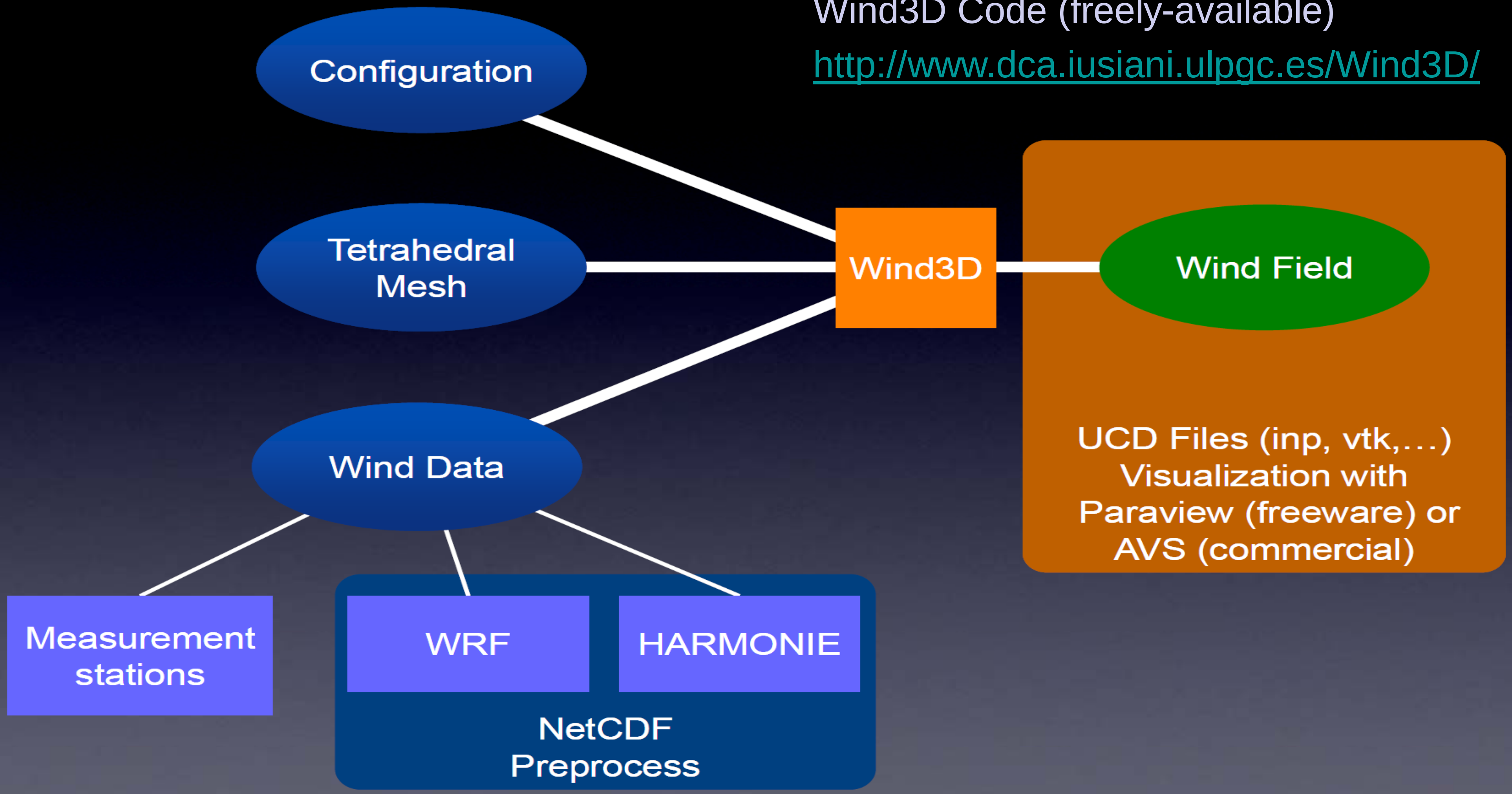

Wind Field Modeling
References

Pergamon

Solar Energy, Vol. 54, No. 1, pp. 49–56, 1995

0038-092X/95 $9.50 + .00

0038-092X(94)00100-6

ADAPTIVE STRATEGIES USING STANDARD AND MIXED FINITE ELEMENTS FOR WIND FIELD ADJUSTMENT

G. WINTER, G. MONTERO, L. FERRAGUT,* and R. MONTENEGRO**

ELSEVIER

Journal of Wind Engineering and Industrial Aerodynamics 89 (2001) 471–488
www.elsevier.com/locate/jweia

Journal of wind engineering and industrial aerodynamics

3-D modelling of wind field adjustment using finite differences in a terrain conformal coordinate system

G. Montero*, N. Sanín

J. Wind Eng. Ind. Aerodyn. 98 (2010) 548–558

Contents lists available at ScienceDirect

ELSEVIER

Journal of Wind Engineering and Industrial Aerodynamics

journal homepage: www.elsevier.com/locate/jweia

Comparison between 2.5-D and 3-D realistic models for wind field adjustment

L. Ferragut [a,*], R. Montenegro [b], G. Montero [b], E. Rodríguez [b], M.I. Asensio [a], J.M. Escobar [b]

ELSEVIER

Journal of Wind Engineering and Industrial Aerodynamics 74–76 (1998) 249–261

Journal of wind engineering and industrial aerodynamics

A 3-D diagnostic model for wind field adjustment

G. Montero[a,*], R. Montenegro[a], J.M. Escobar[b]

ELSEVIER

Advances in Engineering Software 36 (2005) 3–10
www.elsevier.com/locate/advengsoft

ADVANCES IN ENGINEERING SOFTWARE

Genetic algorithms for an improved parameter estimation with local refinement of tetrahedral meshes in a wind model

G. Montero*, E. Rodríguez, R. Montenegro, J.M. Escobar, J.M. González-Yuste

Pure Appl. Geophys. 172 (2015), 109–120

DOI 10.1007/s00024-014-0913-9

Pure and Applied Geophysics

Wind Forecasting Based on the HARMONIE Model and Adaptive Finite Elements

ALBERT OLIVER,[1] EDUARDO RODRÍGUEZ,[1] JOSÉ MARÍA ESCOBAR,[1] GUSTAVO MONTERO,[1] MARIANO HORTAL,[2] JAVIER CALVO,[2] JOSÉ MANUEL CASCÓN,[3] and RAFAEL MONTENEGRO[1]

Objective:

Find the velocity field $\vec{u}(\widetilde{u}, \widetilde{v}, \widetilde{w})$

that adjusts to $\vec{v}_0(u_0, v_0, w_0)$ verifying:

Incompressibility condition in the domain and

No flow-through condition on the terrain

$$\nabla \cdot \vec{u} = 0 \quad \text{in } \Omega$$

$$\vec{n} \cdot \vec{u} = 0 \quad \text{on } \Gamma_b$$

$\Gamma = \Gamma_a \cup \Gamma_b$

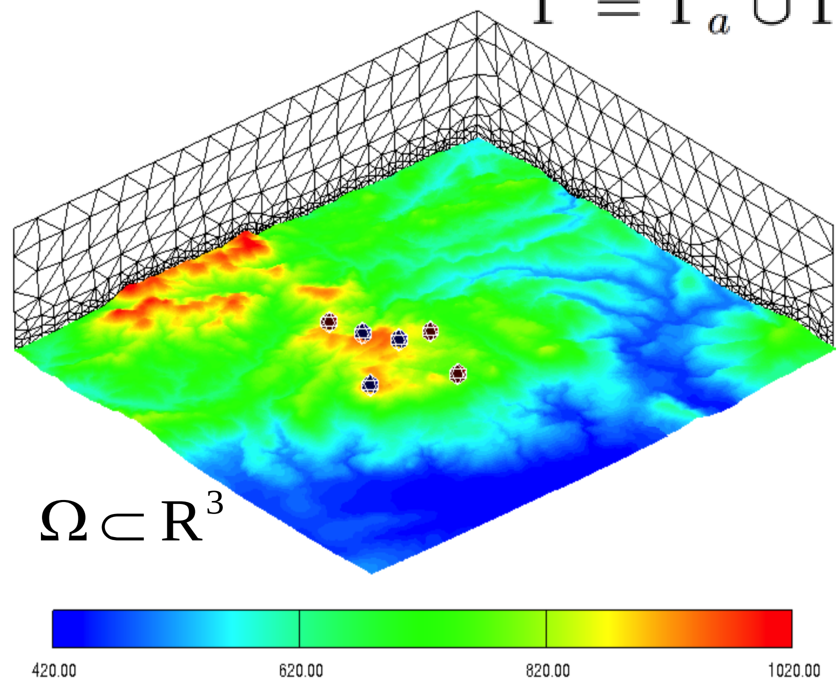

$\Omega \subset R^3$

Let state the least square problem:

$$E(\widetilde{u}, \widetilde{v}, \widetilde{w}) = \int_\Omega [\alpha_1^2\left((\widetilde{u} - u_0)^2 + (\widetilde{v} - v_0)^2\right) + \alpha_2^2(\widetilde{w} - w_0)^2] \ d\Omega$$

$$\alpha = \frac{\alpha_1}{\alpha_2}$$

Gauss Precision Moduli

They allow horizontal (α_1) and vertical (α_2) adjustment of wind velocity components

$\alpha >> 1$ adjustment in vertical direction is predominant

$\alpha << 1$ adjustment in horizontal direction is predominant

$\alpha \rightarrow \infty$ pure vertical adjustment

$\alpha \rightarrow 0$ pure horizontal adjustment

Statement of the problem

To find $\vec{v} \in K$ such that,

$$E(\vec{v}) = \min_{\vec{u} \in K} E(\vec{u}), \quad K = \left\{ \vec{u};\, \vec{\nabla} \cdot \vec{u} = 0,\ \vec{n} \cdot \vec{u}|_{\Gamma_b} = 0 \right\}$$

This problem is equivalent to find the saddle point $(\vec{v}, \phi)$ of the Lagrangian

$$L(\vec{u}, \lambda) = E(\vec{u}) + \int_\Omega \lambda \vec{\nabla} \cdot \vec{u}\, d\Omega$$

with $L(\vec{v}, \lambda) \leq L(\vec{v}, \phi) \leq L(\vec{u}, \phi)$

The solution produces the Euler-Lagrange equations

$\vec{v} = \vec{v}_0 + T\vec{\nabla}\phi$ where $T = (T_h, T_h, T_v)$ $\quad T_h = \dfrac{1}{2\alpha_1^2}$, $T_v = \dfrac{1}{2\alpha_2^2}$

Substituting the Euler-Lagrange equations in

$$\vec{\nabla} \cdot \vec{u} = 0 \quad \text{in } \Omega$$

$$\vec{n} \cdot \vec{u} = 0 \quad \text{on } \Gamma_b$$

it yields the governing equations,

$$-\vec{\nabla} \cdot (T\vec{\nabla}\phi) = \vec{\nabla} \cdot \vec{v}_0 \quad \text{in } \Omega$$

$$\phi = 0 \quad \text{on } \Gamma_a$$

$$\vec{n} \cdot T\vec{\nabla}\phi = -\vec{n} \cdot \vec{v}_0 \quad \text{on } \Gamma_b$$

If Gauss Precision Moduli are constant,

$$\frac{\partial^2\phi}{\partial x^2}+\frac{\partial^2\phi}{\partial y^2}+\alpha^2\frac{\partial^2\phi}{\partial z^2}=-\frac{1}{T_h}\left(\frac{\partial u_0}{\partial x}+\frac{\partial v_0}{\partial y}+\frac{\partial w_0}{\partial z}\right) \quad \text{in } \Omega$$

$$\phi = 0 \quad \text{on } \Gamma_a$$

$$\vec{n}\cdot T\vec{\nabla}\phi = -\vec{n}\cdot\vec{v}_0 \quad \text{on } \Gamma_b$$

Once the Lagrange Multiplier is obtained, the wind velocity is computed with the Euler-Lagrange equations,

$$\vec{v} = \vec{v}_0 + T\vec{\nabla}\phi$$

Wind Field Modeling

Updating of the incomplete Cholesky factorization

The linear system of equations are dependent on $\varepsilon = \alpha^2$,

$$A_\varepsilon x_\varepsilon = b_\varepsilon$$

A suitable preconditioning technique should be applied for an efficient conjugate gradient iteration, in the particular case,

$$A_\varepsilon = M + \varepsilon N$$

So the FEM element matrices are of the form,

$$\{\mathbf{A}^e\}_{ij} = \{\mathbf{M}^e\}_{ij} + \varepsilon \{\mathbf{N}^e\}_{ij}$$

$$A_\varepsilon = (m_{ij}) + \varepsilon (n_{ij}) = \begin{pmatrix} m_{11} + \varepsilon n_{11} & (f_{1M} + \varepsilon f_{1N})^T \\ f_{1M} + \varepsilon f_{1N} & M_2 + \varepsilon N_2 \end{pmatrix}$$

where f_{1M}, f_{1N} are $(n-1) \times 1$ column matrices and M_2, N_2, $(n-1) \times (n-1)$ matrices.

$A_\varepsilon = L_1 Z_1 L_1^T$

$$= \begin{pmatrix} m_{11} + \varepsilon n_{11} & \mathbf{0} \\ l_{1M} + \varepsilon l_{1N} & \mathbf{I} \end{pmatrix} \begin{pmatrix} (m_{11} + \varepsilon n_{11})^{-1} & \mathbf{0} \\ \mathbf{0} & C_2 \end{pmatrix} \begin{pmatrix} m_{11} + \varepsilon n_{11} & (l_{1M} + \varepsilon l_{1N})^T \\ \mathbf{0} & \mathbf{I} \end{pmatrix}$$

Finally,

$$A_\varepsilon \approx L_1 Z_1 L_1^T = L_1 L_2 Z_2 L_2^T L_1^T = (L_1 L_2 \cdots L_n)\, Z_n\, (L_1 L_2 \cdots L_n)^T$$

with Z_i diagonal, $z_{jj} = (m_{jj} + \varepsilon n_{jj})^{-1}$, $j = 1, ..., i$

icholA: Use ICHOL(A_{ε_0}) for all the iterations

icholD: $C_2 = \varepsilon D_2 + M_2 - \dfrac{1}{m_{11}} l_{1M} l_{1M}^T$

icholN: $C_2 = \varepsilon N_2 + M_2 - \dfrac{1}{m_{11}} l_{1M} l_{1M}^T$

fullichol: Comput a new ICHOL decomposition for each ε

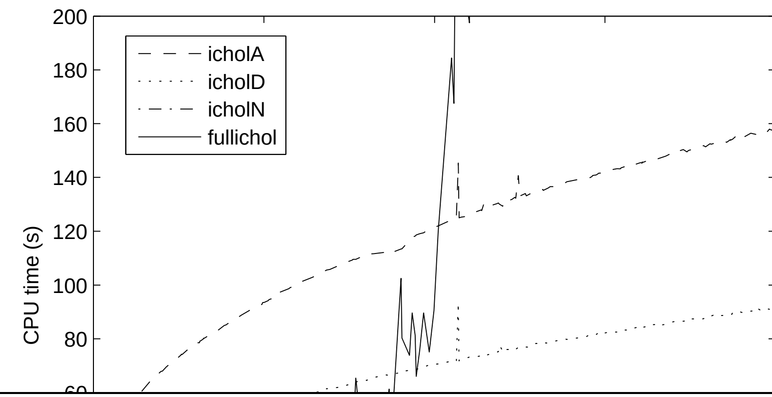

Journal of Computational and Applied Mathematics 235 (2011) 2640–2646

Contents lists available at ScienceDirect

Journal of Computational and Applied Mathematics

journal homepage: www.elsevier.com/locate/cam

Updating incomplete factorization preconditioners for shifted linear systems arising in a wind model

A. Suárez, H. Sarmiento, E. Flórez, M.D. García*, G. Montero

Construction of the observed wind

1. Horizontal interpolation:

    Bilinear Lagrange interpolation from HARMONIE grid wind data

2. Vertical extrapolation (log wind profile):

Stability Classification of the Boundary Layer

(Zilitinkevich, S.S., Tyuryakov, S.A., Troitskaya, Y.I., Mareev, E.A., 2012.)

Table 1: Stability Classification of the Boundary Layer.

Boundary Layer Stability	Surface Buoyancy Flux, B_s $(m^2 s^{-3})$	Squared BL Brunt-Väisälä Frequency, N^2_{h-0} $(s^{-1}$	Free Atmosphere Brunt-Väisälä Frequency, N_{2h-h}	Ratio V_*/W_*
LS (Long-lived Stable)	< 0	≥ 0		
NS (Nocturnal Stable)	< 0	≥ 0		
TN (Truly Neutral)	$= 0$	≥ 0		
CN (Conditionally Neutral)	≥ 0	≥ 0		
PCL (Purely Convective Layer)	> 0	< 0		
MCL (Mechanically Convective Layer)	> 0	< 0		


Journal of Wind Engineering & Industrial Aerodynamics 174 (2018) 411–423

Contents lists available at ScienceDirect

ELSEVIER

Journal of Wind Engineering & Industrial Aerodynamics

journal homepage: www.elsevier.com/locate/jweia

Optimisation technique for improving wind downscaling results by estimating roughness parameters

Gustavo Montero[a], Eduardo Rodríguez[a], Albert Oliver[a,*], Javier Calvo[b], José M. Escobar[a], Rafael Montenegro[a]

SIANI

Vertical extrapolation (log wind profile)

Neutral/Stable Boundary Layer

$$u = \frac{u_*}{k}\left(\ln\frac{\zeta}{\zeta_0} + b_1(\zeta-\zeta_0) + b_2(\zeta-\zeta_0)^2 + b_3(\zeta-\zeta_0)^3\right),$$

$$v = -\frac{u_*}{k}\delta\left(-(\zeta-\zeta_0)\ln(\zeta-\zeta_0) + a_1(\zeta-\zeta_0) + a_2(\zeta-\zeta_0)^2 + a_3(\zeta-\zeta_0)^3\right),$$

$$\zeta = (z-d)/h, \qquad \zeta_0 = z_0/h, \qquad \delta = fh/(ku_*)$$

Convective Boundary Layer

$$|u| = \begin{cases} \frac{u_*}{k}\ln\frac{z-d}{z_0} & z_0 + d < z < \frac{\zeta_u|L|}{k} + d, \\ \frac{u_*}{k}\left[a_u + C_u\left(\frac{k(z-d)}{L}\right)^{-\frac{1}{3}} + \ln\frac{-L}{kz_0}\right] & \frac{\zeta_u|L|}{k} + d \le z \le h, \end{cases}$$

$$\sin\alpha = \sin(\alpha_s - \alpha_{h-0}) = \frac{a_\alpha}{k}\left(\frac{hk}{|L|}\right)^{-\frac{1}{3}}\frac{u_*}{|\overline{u}|}\,\mathrm{sign}\,f,$$

$$|\overline{u}| = |u|_{h-0} = \frac{u_*}{k}\left[a_u + \ln\frac{-L}{kz_0}\right],$$

SIOSE Land Cover Database

Based on

CORINE Land Cover European project

1:25.000 scale

1:100.000 scale

Let l_c be a $n_p \times 1$ vector containing the land cover information of all the points of the studied region, M a $n_p \times 40$ matrix which entries per row are the proportions of basic land covers at each point, and c a 40×1 vector with the basic land cover codes.

$$l_c = Mc = \begin{pmatrix} m_{1,ACM} & m_{1,ACU} & \cdots & m_{1,ZQM} \\ m_{2,ACM} & m_{2,ACU} & \cdots & m_{2,ZQM} \\ \cdots & \cdots & \cdots & \cdots \\ m_{n_p,ACM} & m_{n_p,ACU} & \cdots & m_{n_p,ZQM} \end{pmatrix} \begin{pmatrix} ACM \\ ACU \\ \cdots \\ ZQM \end{pmatrix}$$

such that, for each row i of M, it is verified,

$$\sum_{j=1}^{40} m_{i,j} = 1$$

Roughness length mean

$$z_0 = \prod_{j=1}^{n_b} z_{0j}^{m_{ij}}$$

Displacement height mean

$$d = \sqrt{\sum_{j=1}^{n_b} m_{ij} d_j^2}$$

n_b: number of basic coverages
m_{ij}: fraction of the basic coverage j at the point n_i

Wind Field Modeling

SIOSE Land Cover z_0 and d

Code	Land Cover	z_0 (cm)	z_{0min}–z_{0max}	d (cm)	d_{min}–d_{max}
ACM	Sea Cliff	5[1]	5[2]–19[2]	5700[2]	330[2]–8500[2]
ACU	Water Courses	0.025[3]	0.01[4]–1[5]	0[6,47]	–
AEM	Sheet of Water. Reservoir	0.025[4]	0.01[4]–0.5[7]	0[6,47]	–
AES	Estuaries	0.02[8]	0.01[4]–1[5]	0[6,47]	–
ALC	Coastal Lagoons	0.5[7]	0.01[4]–1[5]	0[6,47]	–
ALG	Sheet of Water. Lakes and Lagoons	0.05[9]	0.01[4]–0.5[7]	0[6,47]	–
AMO	Seas y Oceans	0.02[8]	0.01[4]–3[1]	0[6,47]	–
ARR	Rocky Outcrops and Rocks	0.5[5]	0.03[10]–18[11]	3[6]	0[6]–96[6]
CCH	Screes	10[1]	5[12]–15[13]	60[14]	56[14]–66[14]
CLC	Quaternary lava flow	2.86[15]	0.13[15]–7.35[15]	15[6]	0[6]–40[6]
CNF	Forest. Conifers	128[16]	25[17]–193[18]	1310[19]	487[18]–2200[14]
CHA	Herbaceous crops. Rice	7.2[20]	0.1[21]–11[20]	85[20]	10[20]–155[20]
CHL	Herbaceous crops. Different from Rice	10[22]	0.4[23]–74[24]	25[23]	10[23]–300[35]
EDF	Artificial Coverage. Building	150[26]	70[26]–370[24]	1400[26]	700[26]–1973[6]
FDC	Forest. Leafy. Deciduous	100[28]	18[28]–140[1]	1180[29]	300[29]–2160[29]
FDP	Forest. Leafy. Evergreen	72[11]	60[3]–265[30]	970[29]	300[29]–3100[26]
GNP	No Vegetation. Glaciers and Perpetual Snow	0.1[5]	0.001[31]–1.2[26]	1[6]	0[6]–6[6]

Wind Field Modeling

SIOSE Land Cover z_0 and d

Code	Land Cover	z_0 (cm)	z_{0min}–z_{0max}	d (cm)	d_{min}–d_{max}
HMA	Salt Marshes	11[11]	0.02[10]–17[10]	60[6]	0[6]–93[6]
HPA	Wetlands	10[5	0.5[28]–55[11]	55[6]	3[6]–300[6]
HSA	Continental Salines	1[5]	0.05[5]–4[7]	5[6]	0[6]–22[6]
HSM	Salines	1[5]	0.05[5]–4[7]	5[6]	0[6]–22[6]
HTU	Peat bogs	3[5]	0.05[5]–3[5]	16[6]	0[6]–16[6]
LAA	Artificial Coverage. Artificial Sheet of Water	0.01[5]	0.01[5]–0.5[7]	0[5,47]	–
LFC	Woody Crops. Citrus Fruit Trees	31[33]	3[4]–40[34]	300[14]	0[35]–400[35]
LFN	Woody Crops. No Citrus Fruit Trees	25[5]	3[4]–100[32]	92[36]	0[35]–400[35]
LOC	Other Woody Crops	6.15[37,6]	3.69[37,6]–8.61[37,6]	33[37,6]	20[37,6]–47[37,6]
LOL	Olive Groves	48[38]	25[5]–61[38]	267[38]	200[38]–300[38]
LVI	Vineyards	20[39]	8[40]–55[39]	75[39]	31[40]–140[41]
MTR	Scrubs	16[28]	1.6[28]–100[1]	480[42]	90[26]–710[42]
OCT	Artificial Coverage. Other Buildings	50[5]	6[11]–100[5]	400[27]	200[27]–1400[26]
PDA	No Vegetation. Beaches, Dunes and Sandy Areas	0.03[5]	0.01[43]–6[10]	0[6]	0[6]–33[6]
PRD	Crops. Meadows	3[5]	0.1[31]–10[5]	1.3[26]	0.7[35]–3.5[26]
PST	Grassland	9[31]	0.1[31]–15[31]	17.1[44]	1.3[26]–66[35]
RMB	No Vegetation. Ravine	0.12[45]	0.03[4]–0.5[46]	0.5[6]	0[6]–3[6]
SDN	No Vegetation. Bare Soil	0.1[10]	0.02[46]–4[11]	0.5[6]	0[6]–22[6]
SNE	Artificial Coverage. Unbuilt Land	0.03[10]	0.02[46]–4[1]	0[6]	0[6]–22[6]
VAP	Artificial Coverage. Road, Parking or Unvegetated Pedestrian Areas	3[5]	0.35[45]–50[5]	100[47,48]	2[48]–250[48]
ZAU	Artificial Coverage. Artificial Green Area and Urban Trees	40[4]	3[10]–130[24]	350[47,48]	350[26]–1400[26]
ZEV	Artificial Coverage. Extraction or Waste Areas	10[5]	0.03[10]–18[11]	56[6]	0[6]–100[6]
ZQM	No Vegetation. Burnt Areas	60[5]	10[5]–110[10]	327[6]	54[6]–600[6]

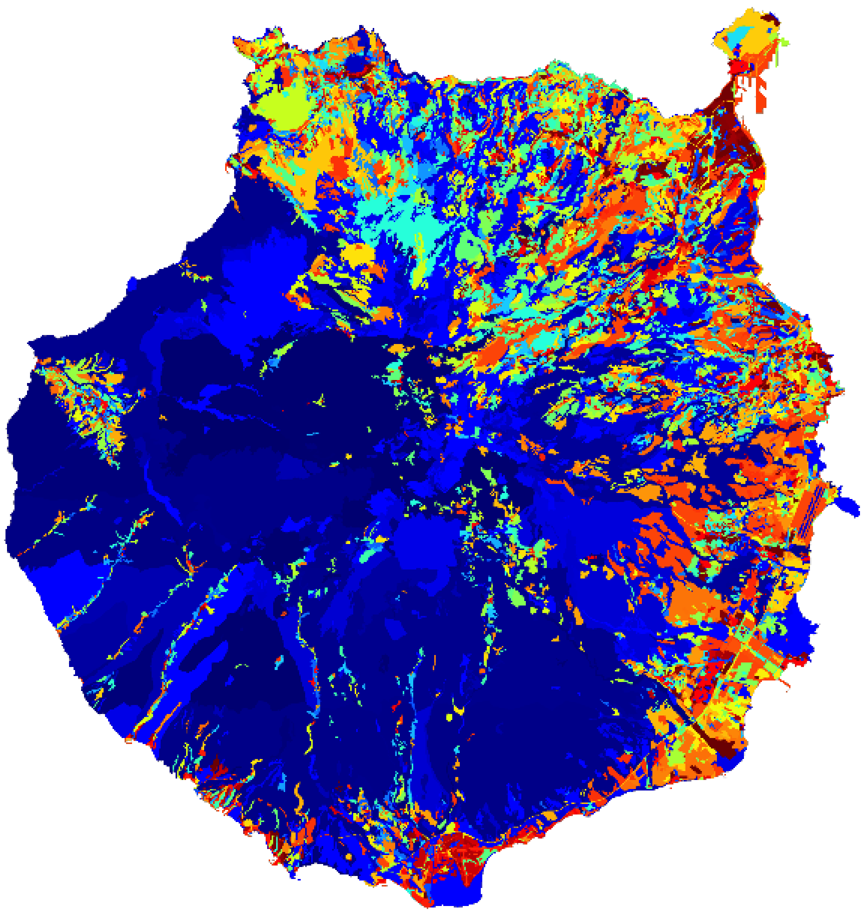

SIOSE Land Cover

Instituto Geográfico Nacional

SIOSE land cover polygons in the Island of Gran Canaria

Roughness length and displacement height of Gran Canaria Island (m)

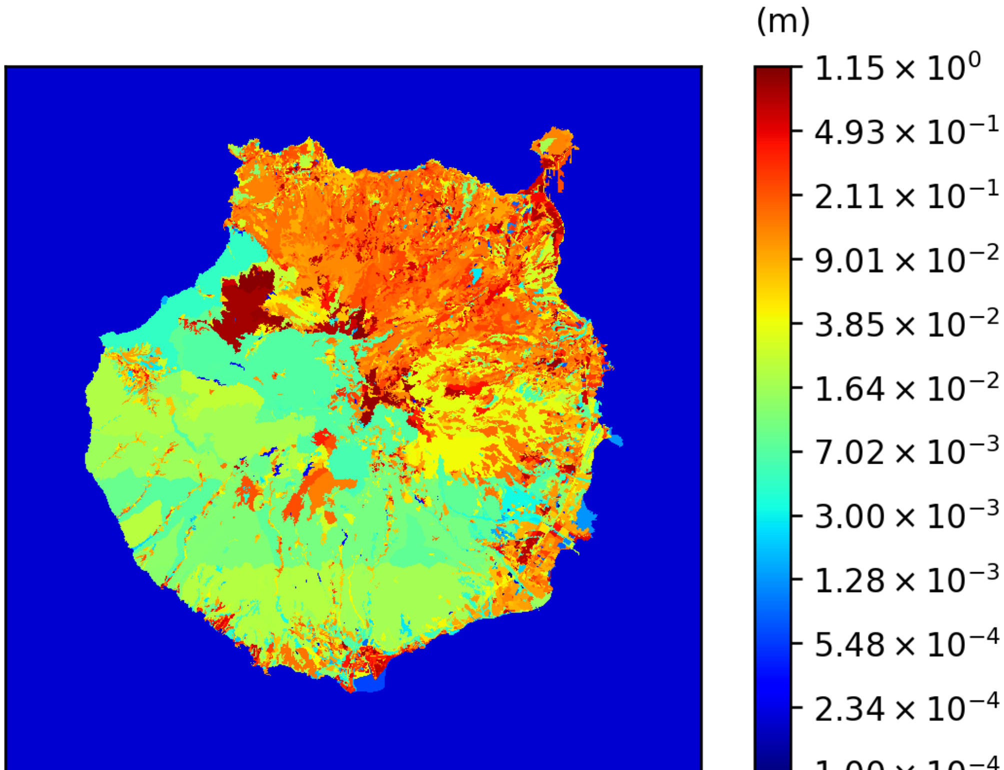

Roughness length (z_0) map

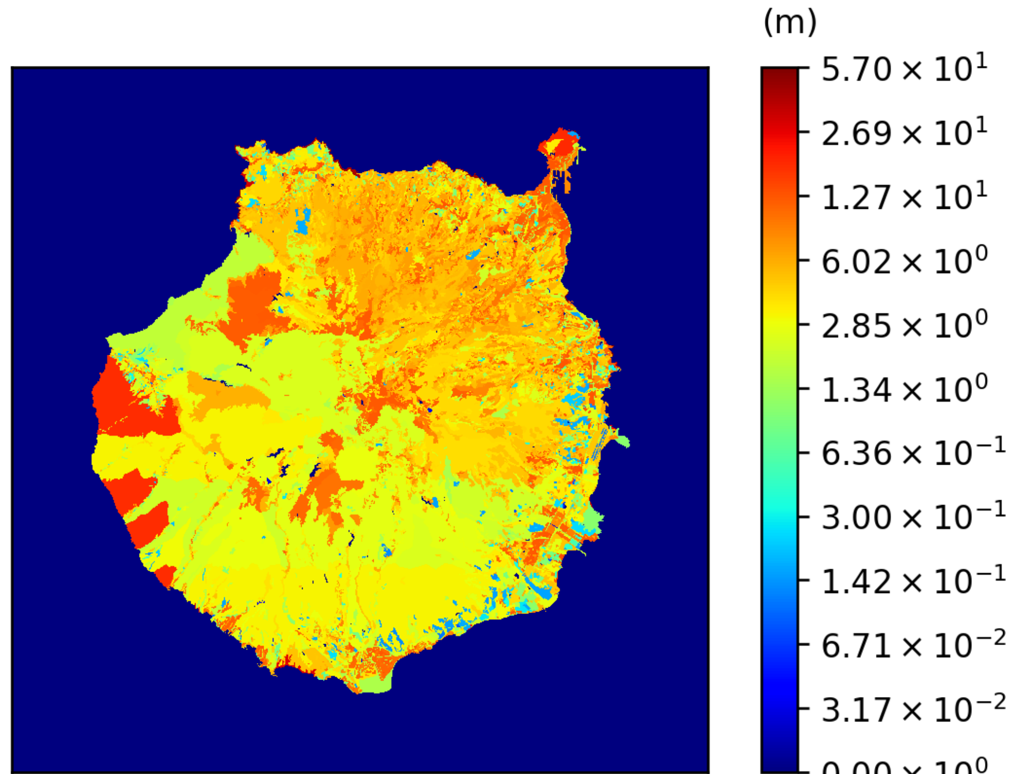

Displacement height (d) map

Differential Evolution

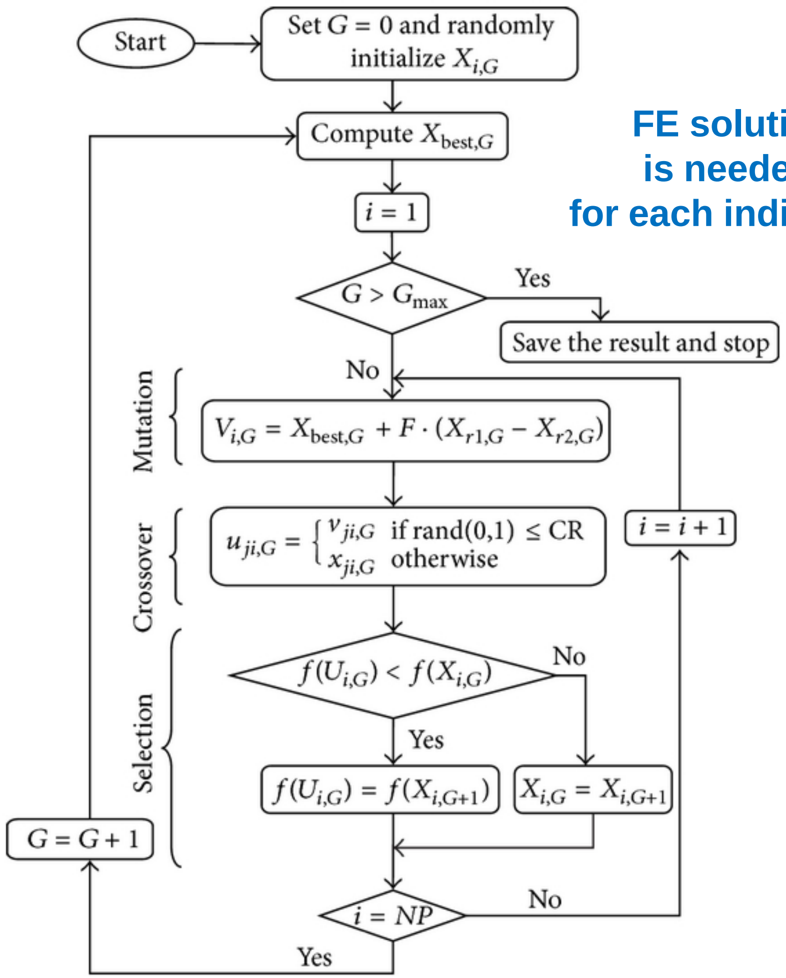

FE solution
is needed
for each individual

$$RMSE = \sqrt{\frac{1}{n_c}\sum_{i=1}^{n_c}(u_{xi} - u_{xi}^c)^2 + (u_{yi} - u_{yi}^c)^2 + (u_{zi} - u_{zi}^c)^2}$$

NE times

Reduction of the search space: Student T distribution

Rebirth: Differential Evolution

L-BFGS-B

SCIPY

Daytime

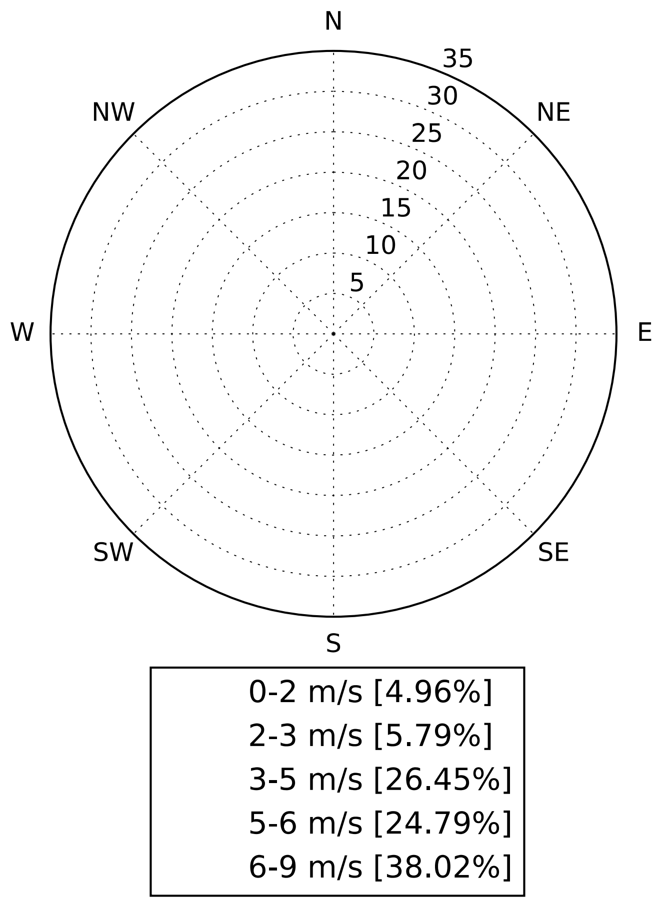

Nighttime

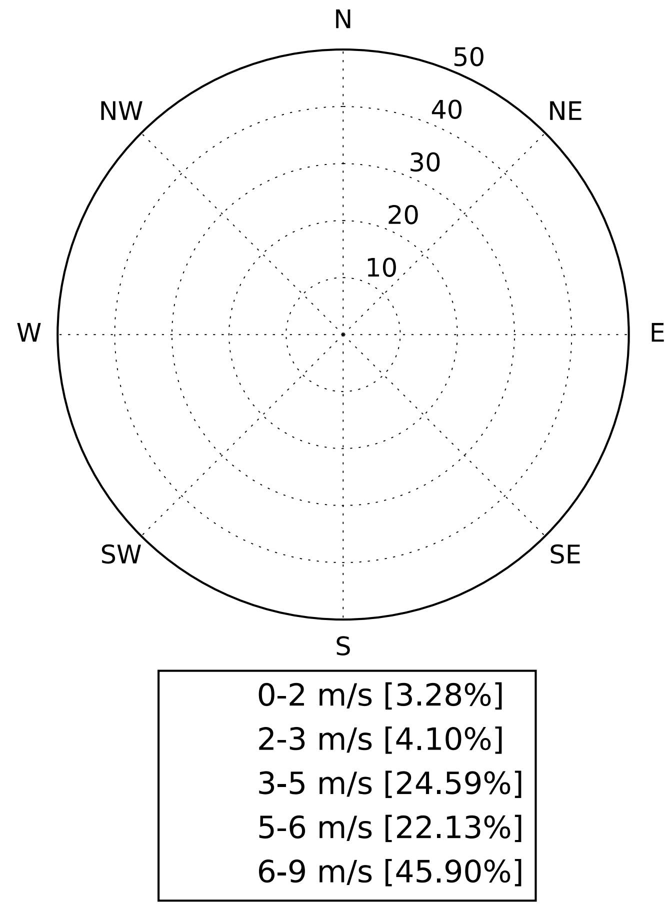

Wind Rose of Gran Canaria at $10\,m$ relating to the period from June 1 to September 30 of the year 2015.

Code	Name	$x\,(m)$	$y\,(m)$	$z\,(m)$
C611E	Vega de San Mateo	442587.00	3094849.87	1712
C612F	Cruz de Tejeda	441111.20	3098128.27	1524
C619I	La Aldea de San Nicolás	420071.67	3097617.70	20
C619X	Agaete	429982.92	3108624.01	15
C619Y	La Aldea	420598.02	3097574.90	23
C623I	S. Bartolomé de Tirajana, Cuevas del Pinar	440978.20	3089240.95	1230
C625O	S. Bartolomé de Tirajana, Lomo Pedro Alfonso	436499.77	3081522.42	816
C628B	La Aldea de San Nicolás, Tasarte	424210.25	3087335.04	328
C629I	Mogán, Puerto	424469.50	3077087.00	22
C629Q	Mogán, Puerto Rico	429927.60	3073056.56	20
C629X	Puerto de Mogán	424751.35	3077101.81	20
C639M	Maspalomas, C. Insular Turismo	443238.31	3070506.07	55
C639U	S. Bartolomé de Tirajana, El Matorral	455345.47	3076502.74	51
C648C	Agüimes	455325.70	3086483.97	316
C648N	Telde, Centro Forestal Doramas	454970.89	3095890.75	354
C649I	Gran Canaria, Aeropuerto	461658.52	3088640.43	34
C649R	Telde, Melenara	462854.84	3095804.64	19
C656V	Teror	446227.23	3105674.70	693
C659H	Polígono de San Cristobal	459130.00	3107201.82	65
C659M	Plaza de la Feria	458627.05	3109809.55	25
C665T	Valleseco	444392.38	3104643.66	910
C669B	Arucas	450225.76	3113015.52	96
C689E	Maspalomas	441057.23	3068075.14	35

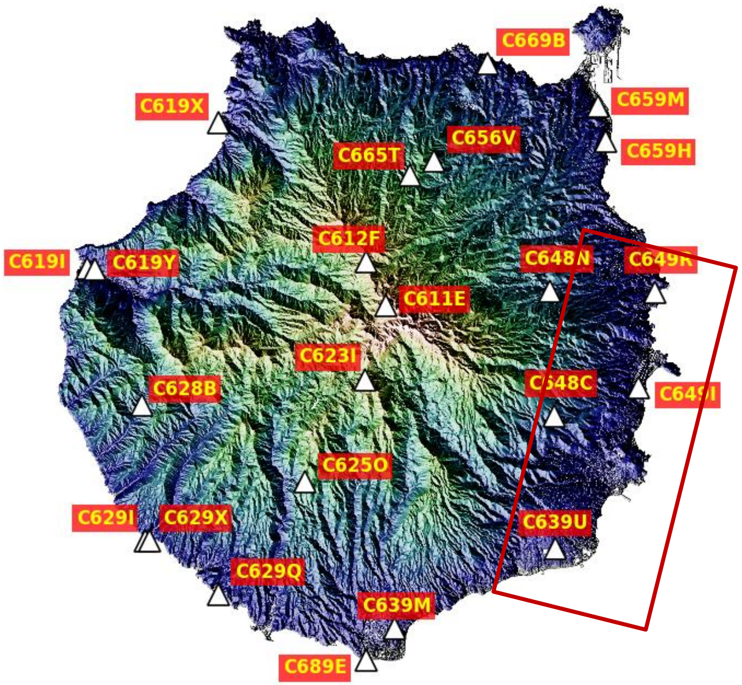

Location in UTM zone 28N coordinates and height over the sea level of the 23 anemometers available in Gran Canaria.

Wind Field Modeling

Adaptive mesh

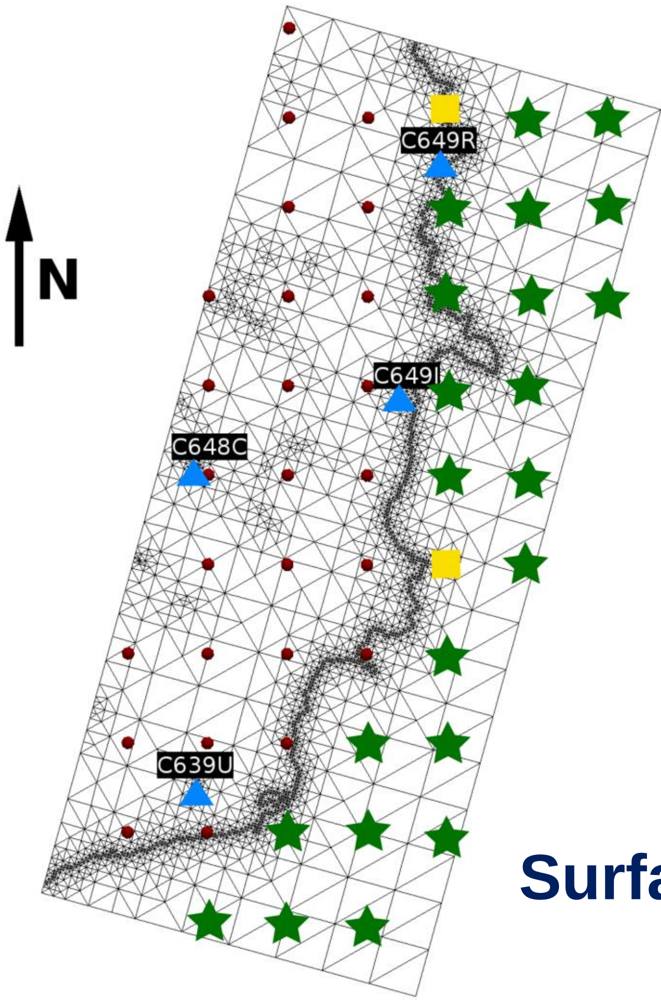

Domain dimensions:
12 km ✕ 28,5 km ✕ 3 km

44.970 tetrahedra
10.070 nodes

Local refinement:
- **Measurement stations**
- **Shoreline**
- **Altimetry**

Surface triangulation

Table 1: Selected wind episodes in an Eastern region of Gran Canaria during June 2015.

BL stability	**HARMONIE 10 m wind speed (ms^{-1})**	**HARMONIE 10 m wind direction ($^\circ$)**	**Surf. buoy. flux, B_s (m^2s^{-3})**	**B-V freq., N_{2h-h} (s^{-1})**	**Ratio V_*/W_***
LS	10.18	336.92 – NNW	-1.38×10^{-4}	1.68×10^{-2}	–
NS	6.10	331.46 – NNW	-9.78×10^{-4}	≈ 0	–
TN	7.51	331.82 – NNW	≈ 0	≈ 0	–
CN	8.52	340.72 – NNW	3.68×10^{-3}	1.04×10^{-2}	–
PC	1.59	116.78 – ESE	6.22×10^{-3}	1.54×10^{-2}	0.17
MC	6.87	358.98 – N	3.02×10^{-3}	1.74×10^{-2}	0.76

Table 1: Location in UTM zone 28N coordinates and heights above the sea level of the anemometers used in the numerical application in Gran Canaria Island.

Code	**Name**	$\boldsymbol{x}$ (m)	$\boldsymbol{y}$ (m)	$\boldsymbol{z}$ (m)
C639U	San Bartolomé de Tirajana, El Matorral	455345	3076503	51
C648C	Aguimes	455326	3086484	316
C649I	Gran Canaria, Aeropuerto	461659	3088640	34
C649R	Telde, Melenara	462855	3095805	19

Table 1: Experiment results with data from HARMONIE-AROME and ECMWF.

Wind direction	**NNW**	**NNW**	**NNW**	**NNW**	**N**	**N**
Wind speed (ms^{-1})	$v > 6$	$v > 6$	$v > 6$	$v > 6$	$v \leq 2$	$v > 6$
Stability	**LS**	**NS**	**TN**	**CN**	**PC**	**MC**
RMSE(H-A)	8.47	3.12	5.94	7.89	3.29	2.46
RMSE(H-A/W3D) nominal values	4.00	3.47	4.74	6.21	2.55	2.40
RMSE(H-A/W3D) estimated values	2.44	2.59	3.47	4.78	2.27	1.31
RMSE(ECMWF)	7.08	3.88	3.16	6.14	2.97	2.98
RMSE(ECMWF/W3D) nominal values	4.00	3.47	4.74	6.21	2.55	5.90
RMSE(ECMWF/W3D) estimated values	2.56	2.91	3.68	4.79	2.53	2.35

Wind Field Modeling

Results for 2 selected cases: improvements on NWP forecasting

LS Boundary Layer

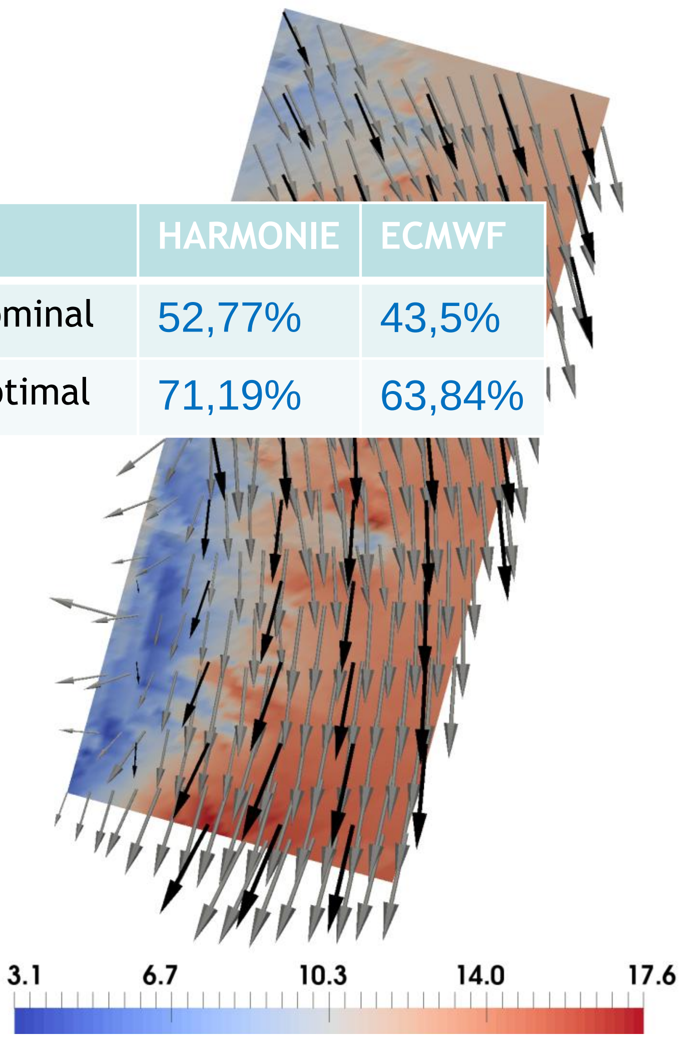

LS	HARMONIE	ECMWF
WIND-3D - Nominal	52,77%	43,5%
WIND-3D - Optimal	71,19%	63,84%

MC Boundary Layer

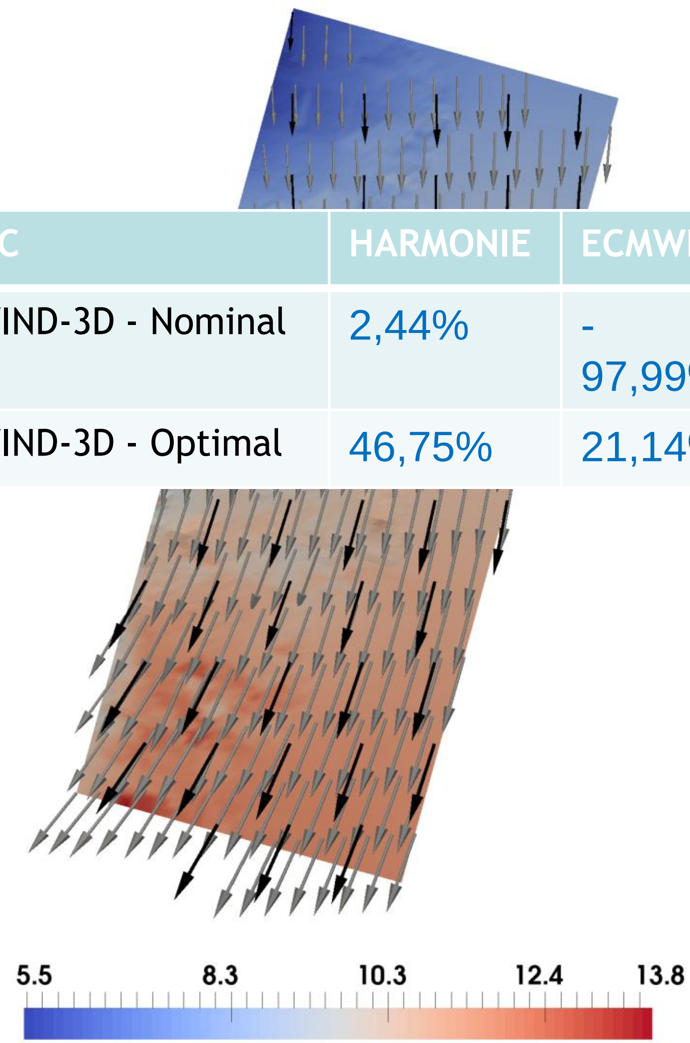

MC	HARMONIE	ECMWF
WIND-3D - Nominal	2,44%	-97,99%
WIND-3D - Optimal	46,75%	21,14%

Conclusions

- Mass Consistent models (MCM) can improve the forecasting results of Mesoscale models
- The studied parameters involved in MCM depend on the wind velocity (speed and direction), and the atmospheric stability. Also day-time and night-time results are different.
- The mimetic algorithm proposed is a robust tool for solving this type of parameter estimation problems.

Future Research

- Construct a reduced basis of those parameters for solving wind episodes (different locations). Only forecasting values as input data.
- Apply this methodology to the results of different mesoscale models (HARMONIE, ECMWF)
- Reproduce the study with a mass and momentum conserving model.